ISSN 1063-7729, Astronomy Reports, 2023, Vol. 67, Suppl. 2, pp. S179–S188. © Pleiades Publishing, Ltd., 2023.

Plausible Detection of Rotating Magnetized Neutron Stars by Their Continious Gravitational Waves[1]

Mayusree Das[a],* and Banibrata Mukhopadhyay[a]

[a]*Joint Astronomy Programme, Department of Physics, Indian Institute of Science, Bangalore, 560012 India*

** e-mail: mayusreedas@iisc.ac.in*

Received September 30, 2023; revised November 21, 2023; accepted November 21, 2023

Abstract—In the past decades, several neutron stars (NSs), particularly pulsars, with mass $M > 2M_{\odot}$, have been observed. Hence, there is a generic question of the origin of massive compact objects. Here we explore the existence of massive, magnetized, rotating NSs by solving axisymmetric stationary stellar equilibria in general relativity using the Einstein equation solver for stellar structure *XNS* code. Such rotating NSs with magnetic field and rotation axes misaligned, hence with non-zero obliquity angle, can emit continuous gravitational waves (GW). We discuss the decay of the magnetic field due to Ohmic, Hall and Ambipolar diffusion, and the decay of angular velocity, and obliquity angle with time due to angular momentum extraction by GW and dipole radiation, which determine the timescales related to the GW emission. Further, in the Alfvén timescale, a differentially rotating, massive proto-NS rapidly settles into a uniformly rotating, less massive NS due to magnetic braking and viscosity. These explorations suggest that detecting massive NSs is challenging and sets a timescale for detection. We calculate the signal-to-noise ratio of GW emission, which confirms that any detector cannot detect them immediately, but detectable by Einstein Telescope and Cosmic Explorer over months of integration time, leading to direct detection of NSs.

Keywords: gravitational waves, neutron stars, magnetic stars, gravitation, astronomical radiation sources, gravitational wave sources, pulsars, stellar magnetic fields

DOI: 10.1134/S1063772923140056

1. INTRODUCTION

Since the first direct evidence for gravitational wave (GW) emission in 2015, there have been many subsequent discoveries of GW emissions, mostly from binary mergers detected by LIGO and VIRGO [1, 2]. We know that the binary systems possess time-varying quadrupole moment while merging, when their all three principal moments of inertia are different, which results in emitting GW from them. However, isolated objects with misaligned magnetic and rotation axes (obliquity angle non-zero) may also have non-zero time-varying quadrupole moment. Therefore, they should also emit GW continuously, unlike transiently in a binary, called continuous GW (CGW) [3]. Nevertheless, there is no CGW detected from any isolated object yet in aLIGO, and aVIRGO [4], even though many neutron stars (NSs) are inferred to be rotating and magnetized which generally should have non-zero obliquity angle [5] and may be adequate enough for the detectable CGW amplitude. What is the short-fall: underlying models or observational/detectional limitations or combination of them? In this paper, we explore the time varying properties of isolated NSs to understand their delection possibility in CGW. However, the obliquity angle is expected to be evolved with time as a pulsating NS emits electromagnetic as well as gravitational radiation. In this work, we study the time evolutions of magnetic field, rotational frequency and obliquity angle of an isolated NS. We plan to discuss the model of the pulsating, magnetized compact object radiating GW and show the output models of NSs from *XNS* code in Section 2. Then we discuss how GW amplitude decreases due to spin-down (along with alignment of axes) in Section 3. In Section 4, we calculate corresponding signal to noise ratio (SNR) and discuss the timescales for detecting them. Finally we end with conclusions in Section 5.

2. CGWS FROM PULSATING COMPACT STARS AND SAMPLE MODELS

For a star with angular frequency Ω, obliquity angle χ and the angle between the rotation axis of the object

[1] Paper presented at the Fifth Zeldovich meeting, an international conference in honor of Ya.B. Zeldovich held in Yerevan, Armenia on June 12–16, 2023. Published by the recommendation of the special editors: R. Ruffini, N. Sahakyan and G.V. Vereshchagin.

and our line of sight i, the strain of the two polarizations of the GW at any time t is given by [3, 5]

$$h_+ = h_0 \sin\chi\left[\frac{1}{2}\cos i \sin i \cos\chi \cos\Omega t - \frac{1+\cos^2 i}{2}\sin\chi\cos 2\Omega t\right],$$

$$h_\times = h_0 \sin\chi\left[\frac{1}{2}\sin i \cos\chi \sin\Omega t - \cos i \sin\chi \sin 2\Omega t\right].$$

Here, $h_0 = (4G/c^4)(\Omega^2 \epsilon I_{xx}/d)$, for $\chi \to 0$ (but $\neq 0$), where c is the speed of light, G is Newton's gravitational constant, d is the distance between the detector and the source object, and the ellipticity is defined as $\epsilon = |I_{zz} - I_{xx}|/I_{xx}$, where I_{xx} and I_{zz} are the principal moments of inertia of the star about x- and z-axes, respectively. An object behaving as a pulsar can emit CGWs at two frequencies, Ω and 2Ω.

The properties of the star in the above CGW polarizations and amplitude are encapsulated in I_{xx}, I_{zz}, Ω, and χ. In order to model the underlying NSs, we use the publicly available *XNS* code,[2] which is the Einstein equation solver for a NS with varieties of properties [6].

The equations describing stellar structure require an equation of state (EoS) which, however, has to be supplied in the polytropic form, i.e., as $\mathcal{P} = K\rho^\Gamma$ for the purpose of *XNS* solution, where $\mathcal{P}$ is the pressure, ρ the density, Γ the polytropic index, and K the polytropic constant. We will choose $\Gamma = 1.95$, $K = 11.3 \times 10^5$ cm^5 g^{-1} s^{-2} for this work.

Moreover, the code does not have information about the obliquity angle. However if χ is actually zero, the star does not radiate GW. Thus, we make small χ approximation in our computations related to CGW based on the *XNS* outputs. Note that the amplitudes of h_+ and $h_\times$ in Eq. (1) will be further suppressed by other factors. For example, at $\chi = 3°$, $\max[\sin\chi\{(1/2)\cos i \sin i \cos\chi\cos\Omega t - ((1+\cos^2 i)/2)\sin\chi\cos 2\Omega t\}] = 0.0110297$ for $t = 0$ and $i = i_{\max} \approx 46.5°$. Therefore, the maximum CGW amplitude from a star with $\chi = 3°$ received by the detector is $h = 0.0110297 h_0$, which we consider in our computations. The amplitude of GW also depends on the distance d between the source and the detector. We consider $d = 10$ kpc.

We depict a typical rotating toroidal field dominated NS from our simulation in Fig. 1 (top panel). Notice the density contour, indicating that while inner region is prolate due to toroidal magnetic field, with increasing radius as field decays the effect goes off. However, the rotational effect makes the star oblate, leading to a competition between these two opposing effects which determines the overall shape of the star. In the outer region, the centrifugal term dominates and the shape becomes (slightly) oblate. As the relative strength between toroidal magnetic field and angular frequency determines the overall shape, increasing magnetic field deviates the star more from spherical geometry, which produces higher quadrupole moment and, thus, higher ellipticity. As a result this leads to higher h_0 as $h_0 \propto \epsilon$. The same goes with angular frequency as $h_0 \propto \Omega^2$. Figure 1 (bottom panel) captures the magnetic field configuration for the same star.

A poloidal magnetic field and rotational effect act in the same direction in the NS making it an oblate spheroid, as shown in Fig. 2 (top panel). Unlike the toroidally dominated case, here throughout the star remains oblate. This is because effect of rotation remains uniform throughout the star, even though the field decays with radius. Figure 2 (bottom panel) depicts the corresponding field configuration.

3. EVOLUTIONS OF SPIN AND OBLIQUITY ANGLE

A triaxial magnetized NS behaving as a pulsar will emit dipole and gravitational radiations simultaneously, which respectively lead to the dipole and quadrupolar luminosities. The angular frequency of pulsating NS decreases with time due to its emitting gravitational and electromagnetic dipole radiations which in turn leads to the extraction of angular momentum. This further results in the change in the obliquity angle as they are coupled. For an oblique rotator, the evolutions for Ω and χ involve with the GW radiation and electromagnetic energy-loss terms [7, 8] given by

$$\frac{d(\Omega I_{z'z'})}{dt} = -\frac{2G}{5c^5}(I_{zz} - I_{xx})^2\Omega^5 \sin^2\chi(1+15\sin^2\chi) - \frac{B_p^2 R_p^6 \Omega^3}{2c^3}\sin^2\chi F(x_0), \quad (1)$$

and

$$I_{z'z'}\frac{d\chi}{dt} = -\frac{12G}{5c^5}(I_{zz} - I_{xx})^2\Omega^4 \sin^3\chi\cos\chi - \frac{B_p^2 R_p^6 \Omega^2}{2c^3}\sin\chi\cos\chi F(x_0), \quad (2)$$

where $F(x_0) = (x_0^4/5(x_0^6 - 3x_0^4 + 36)) + (1/3(x_0^2+1))$, $x_0 = R_0\Omega/c$, B_p is the strength of the magnetic field at the pole, R_p is poler radius, R_0 is the average radius of the star.

In order to understand the evolution of a pulser, e.g. how long a NS could behave as a pulsar, we have to solve the set of Eqs. (1) and (2). To solve Eqs. (1) and (2), the various quantities, such as I_{xx}, I_{zz}, B_P, and R_P, at the initial time are supplied as the output of a

[2] https://www.arcetri.inaf.it/science/ahead/XNS/code.html

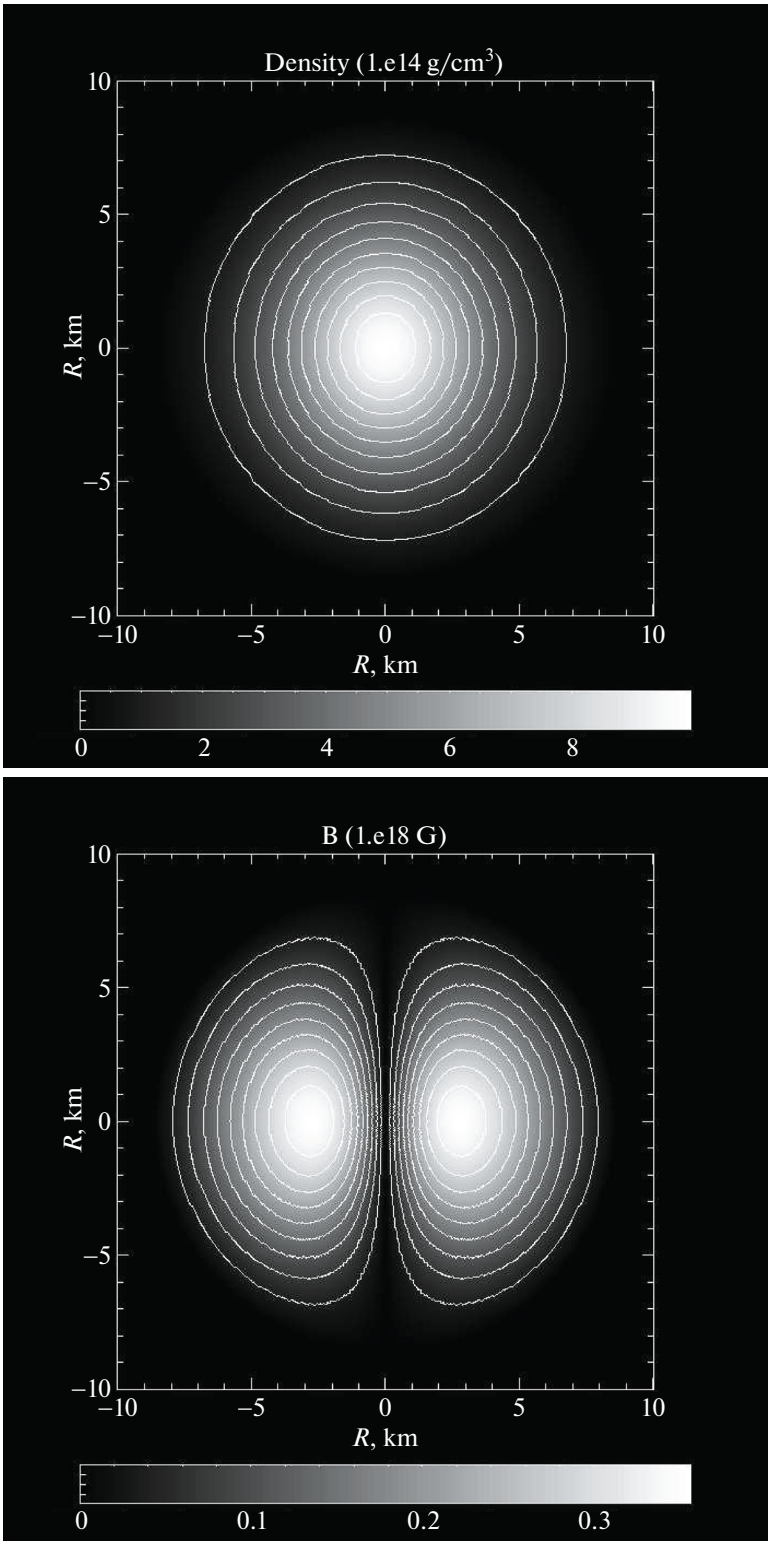

Fig. 1. Density isocontours (top panel) and magnetic field lines (bottom panel) of uniformly rotating toroidally magnetized NS of mass $M = 1.91M_\odot$ with $\nu = 200$ Hz, $B_{\max} = 3.5\times10^{17}$ G, ME/GE $= 3\times10^{-2}$ and KE/GE $= 6.6\times10^{-3}$.

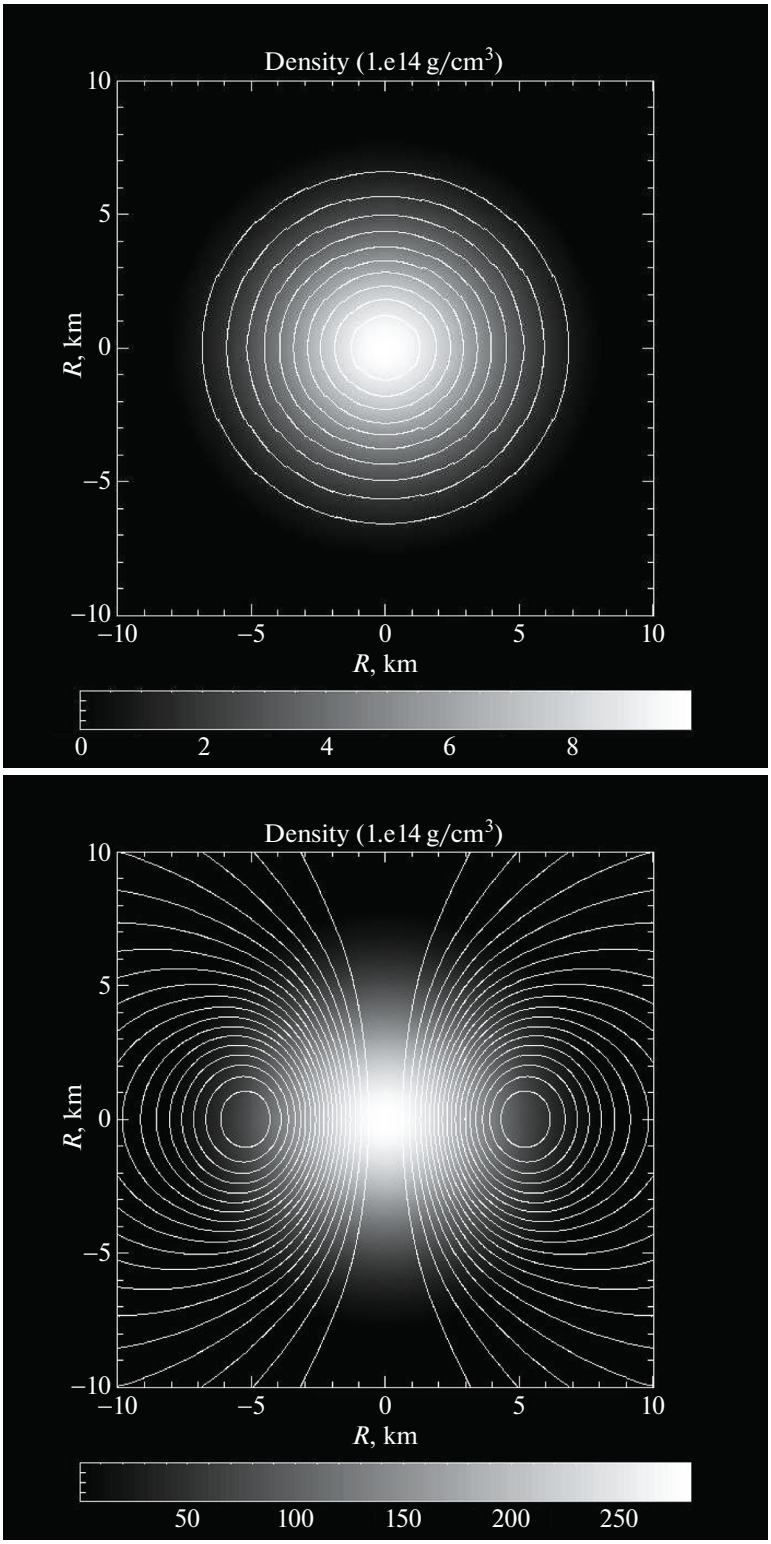

Fig. 2. Density isocontours (top panel) and magnetic field lines (bottom panel) of uniformly rotating poloidally magnetized NS of mass $M = 1.91M_{\odot}$ with $\nu = 50$ Hz, $B_{\max} = 3.5\times10^{17}$ G, ME/GE $= 1.3\times10^{-2}$ and KE/GE $= 2\times10^{-4}$.

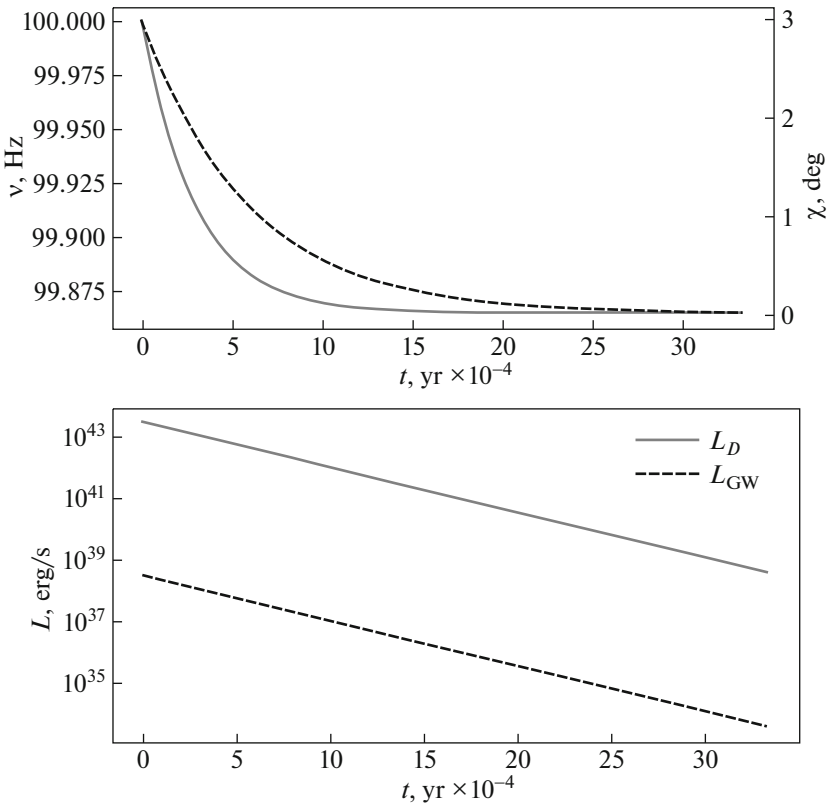

Fig. 3. $L_D \gg L_{\rm GW}$: Variations of ν, χ, $L_{\rm GW}$ and L_D with time for $B_P = 2\times10^{15}$ G, initial $\nu = 100$ Hz, $\chi = 3°$ (Ref: Table 1).

NS model from the *XNS* code. We choose a star with the initial $\chi = 3°$ along with two B_p. Therefore, from Eqs. (1) and (2) we can explore the timescales for purely poloidally (or poloidally dominated) magnetized NSs behaving as pulsars, assuming the NSs to be oscillating/rotating dipoles.

Highly poloidally magnetized NSs should have $L_D \gg L_{\rm GW}$, when L_D governs the timescale. In this case, χ becomes 0 very fast, and NS starts rotating with a different angular frequency than its original value, as shown by Fig. 3. Simultaneously, L_D and $L_{\rm GW}$ also decay as shown in the same figure. For a NS with high poloidal field, of $B_P = 2\times10^{15}$ G, the χ decays in timescale of days. Due to very fast decays of χ and L_D, this NS cannot emit radiation for a long. Therefore, it will be very difficult to detect such NSs by the future GW detectors (or they may easily be missed to be detected) or they may be detected just for a very short duration of time.

At a lower poloidal magnetic field, $L_{\rm GW} \gg L_D$. In such a case, luminosity decreases slowly, and the NS can radiate for a longer period. χ and Ω decay simultaneously for a long time before approaching zero and a saturated value, respectively (see Fig. 4). This further leads $L_{\rm GW}$ and L_D to remain higher for longer. Naturally, in this case, the decays of χ and Ω are governed by GW radiation mainly. For a NS of $B_P = 2\times10^{12}$ G (Table 1), χ decays in a much longer timescale, which is 10^3 yr.

We consider a few NSs with purely toroidal magnetic fields (as toroidally dominated stars). We further drop the contribution of L_D from Eqs. (1) and (2), assuming that even if the NS possesses any dipole contribution, its effect is much smaller than the other contribution. As a result, here $L_{\rm GW} \gg L_D$. Such a magnetized massive NS can radiate for a long time. However, detecting such NSs by the GW detector and the duration of detection are determined by the (relative) strengths of the toroidal and poloidal field components. As the stable mixed field configuration has been argued to be toroidally dominated [9], the above mentioned configuration remains stable even after a long time. These NSs will be detectable by GW detectors for a longer duration, as understood by Fig. 5 when $L_{\rm GW}$ remains high for a longer duration. The underlying GW amplitude is listed in Table 2 at $t = 0$ which, however, will decay with time due to evolutions of χ and Ω.

Table 3 and Fig. 6 show then that the GW amplitude for toroidally dominated NS, which is a function

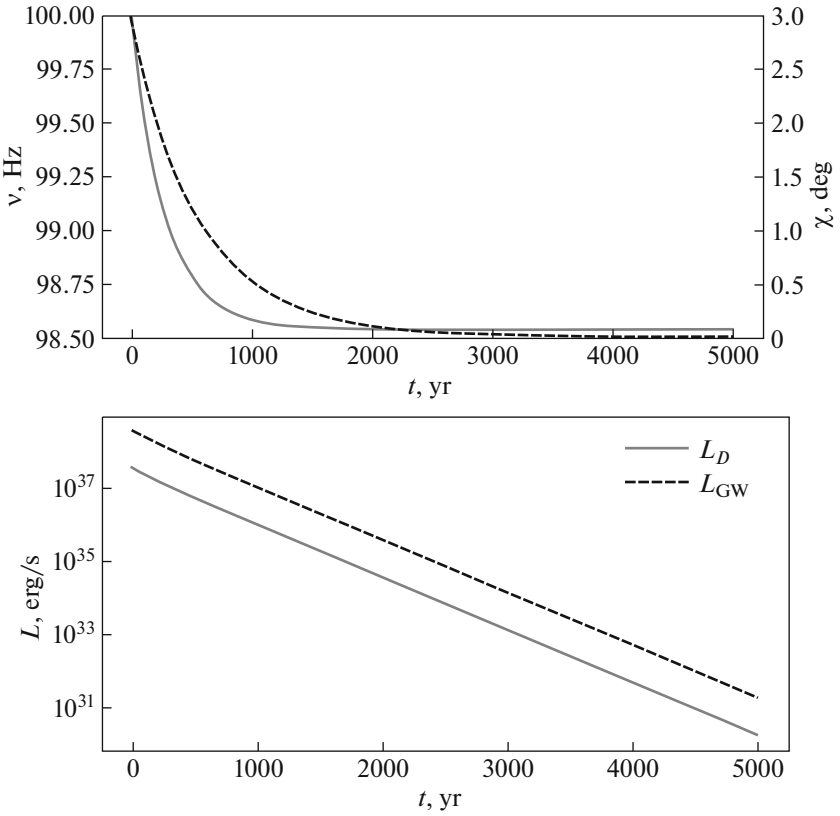

Fig. 4. $L_{GW} \gg L_D$: Variations of ν, χ, L_{GW} and L_D with time for $B_P = 2\times10^{12}$ G, initial ν = 100 Hz, χ = 3° (Ref: Table 1).

of χ and Ω, decays with time. Figure 6 shows that while the GW amplitude for a NS at its birth was detectable by some detectors, e.g., Einstein Telescope and Cosmic Explorer, after some time it goes below the detectable limit.

4. SENSITIVITY OF CGW DETECTORS

The question arises, how to increase the signal to noise ratio (SNR) so that CGW from NSs can be detected which otherwise seems to be going quickly below the sensitivity limit of the detectors. Indeed, an extensive effort is going on to increase the sensitivity of detectors by calculating SNR to detect CGWs from various sources [10]. This can be done by estimating the necessary observation time for the particular GW detector to detect these objects. Subsequently, the cumulative SNR of the detector can be calculated coherently by discretizing the timescale finely, including information about phase for each grid. However, as discussed above that the NS spins down fast so that ν and χ change rapidly, resulting in GW strain also changing fast. Therefore, the time integration for entire time T should be accomplished by time-stacks

Table 1. Uniformly rotating NSs with the poloidal magnetic field, where $\rho_c = 10^{15}$ g cm^{-3}, and ν = 100 Hz at $t = 0$. Here M denotes the mass, R_E the equatorial radius, R_P the polar radius, B_{max} the maximum magnetic field, ME, KE, and GE are respectively magnetic, kinetic and gravitational energies of the star, $\nu = \Omega/2\pi$. I_{xx} and I_{zz} are in the units 4.5×10^{43} g cm^2

M ($M_\odot$)	R_P, km	B_P, G	ME/GE	KE/GE	I_{xx}	I_{zz}	L_{GW}, erg/s	L_D, erg/s	h_0 (d = 10 kpc)
1.93	11.5	5.5×10^{16}	1.3×10^{-2}	7.9×10^{-4}	10.99	11.46	8.5×10^{40}	1.8×10^{46}	8.2×10^{-23}
1.9	11.99	2×10^{15}	1.6×10^{-5}	7.7×10^{-4}	11.409	11.438	3.5×10^{38}	3.1×10^{43}	6×10^{-24}
1.9	11.99	2×10^{12}	1.8×10^{-11}	7.7×10^{-4}	11.409	11.439	3.5×10^{38}	3.1×10^{37}	2×10^{-25}

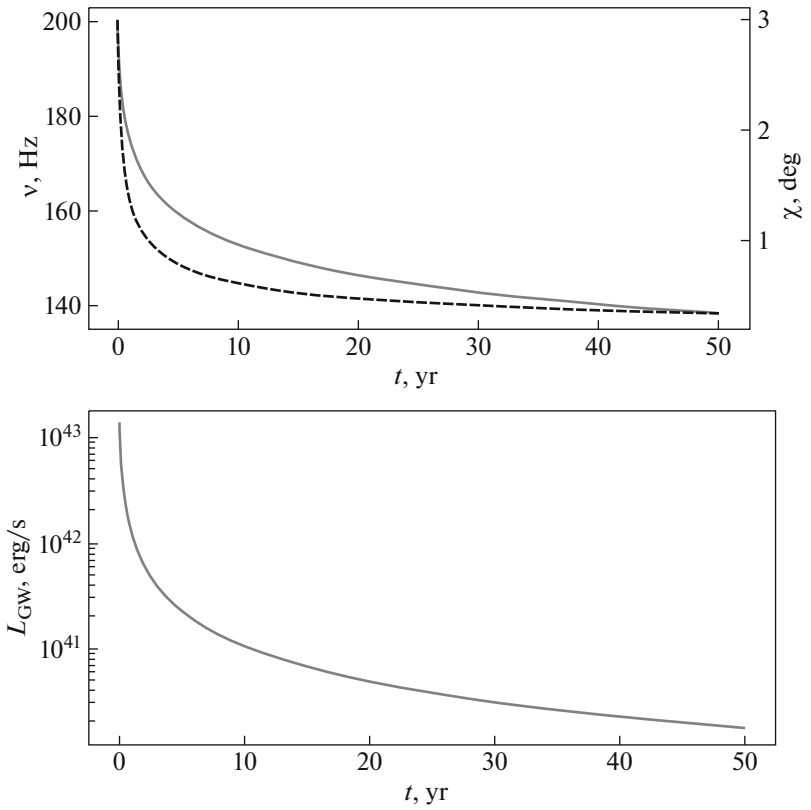

Fig. 5. For toroidally dominated NSs: Variations of ν, χ, and $L_{\rm GW}$ as functions of time for $B_{\rm max} = 3.5\times10^{17}$ G, initial $\nu = 200$ Hz, $\chi = 3°$ (Ref: Table 2).

$T_{\rm stack}$ such that, in each $\mathcal{N}$th stack, ν and χ remain nearly constant, and $T = \mathcal{N}T_{\rm stack}$. For each stack, SNR is calculated coherently and then added incoherently to obtain the cumulative SNR. An incoherent search with a time-stacking method is computationally efficient compared to the coherent search [11, 12]. Assuming ν, χ and h_0 remain nearly constant over each time-stack, adding $\mathcal{N}$ such stacks, the cumulative SNR is given by [13]

$$\langle S/N\rangle = \sqrt{\frac{\sin^2\zeta}{100}\frac{h_0^2 T\sin^2 2\chi}{\sqrt{\mathcal{N}}S_n(\nu)} + \frac{4\sin^2\zeta}{25}\frac{h_0^2 T\sin 4\chi}{\sqrt{\mathcal{N}}S_n(2\nu)}}, \quad (3)$$

where ζ is the angle between the interferometer arms and $S_n(\nu)$ is the power spectral density (PSD) of detector at the frequency ν [14, 15]. For ground-based interferometers such as LIGO, VIRGO, KAGRA, Cosmic Explorer, etc. $\zeta = 90°$ and for space-based interferometers such as Einstein Telescope $\zeta = 60°$. The averaging is done over all possible angles, including i, which determines the orientation of the object with respect to the references frame of celestial sphere. Here we consider $T_{\rm stack} \approx 3$ hr. We set the threshold value for SNR to be 12 for more than 96% detection efficiency [1].

Table 2. Uniformly rotating NSs with the toroidal magnetic field, where $\rho_c = 10^{15}$ g cm^{-3} at $t = 0$. The rest is the same as Table 1

M ($M_\odot$)	R_E, km	$B_{\rm max}$, G	ν, Hz	ME/GE	KE/GE	I_{xx}	I_{zz}	$L_{\rm GW}$, erg/s	h_0 ($d = 10$ kpc)
1.963	13.31	3.5×10^{17}	500	3.3×10^{-2}	2×10^{-2}	12.75	12.84	5×10^{43}	4.2×10^{-21}
1.91	12.65	3.5×10^{17}	200	3.2×10^{-2}	6.6×10^{-3}	12.81	12.08	1.32×10^{43}	6.7×10^{-22}
1.909	12.15	1.2×10^{17}	200	3.3×10^{-3}	3.1×10^{-3}	11.53	11.57	4×10^{40}	6×10^{-23}

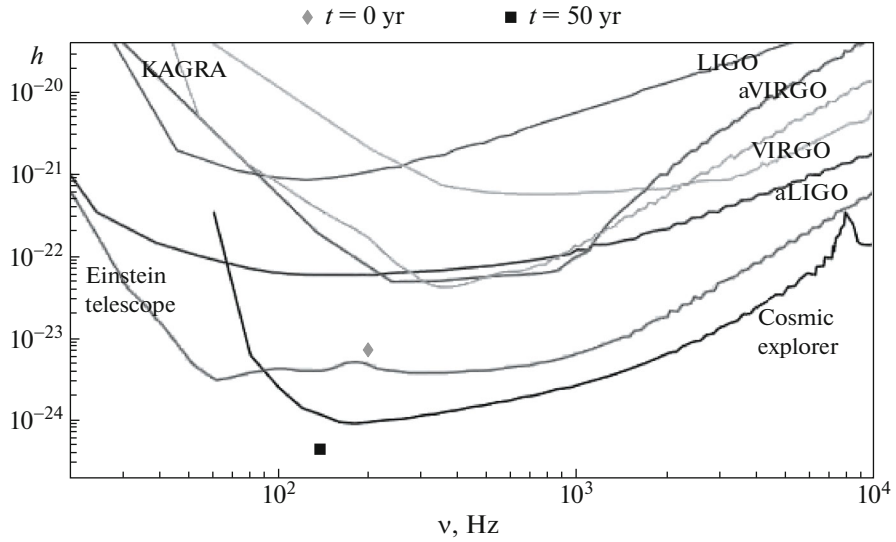

Fig. 6. Dimensionless GW amplitudes for NSs before and after ν and χ decay along with the sensitivity curve of various detectors for $B_{\max} = 3.5\times10^{17}$ G, initial ν = 200 Hz, χ = 3° (Ref: Table 3).

Figure 7 shows the SNR as a function of time with different field strengths. We assume the toroidal field based NSs as toroidal dominated stars with a negligible poloidal surface field with respect to the maximum toroidal field $B_{\max}$. Such a poloidal field does not change the shape and size of the NS practically. As L_D is small, Ω and χ hardly change within 1 yr. We show SNR in Fig. 7 for $B_{\max} = 3.5\times10^{17}$ G and 1.2×10^{17} G. While for the stronger field, Cosmic Explorer will be able to detect it in some months of integration, for the weaker field, it will take longer to detect, this is because, as the field strength decreases, SNR decreases, as shown in Fig. 7.

5. CONCLUSIONS

After the detection of GW from the merger events, there is a great interest in the scientific community to discover CGW from isolated NSs. In the future, highly magnetized, rotating, massive NSs may be detected by Einstein Telescope, which will confirm a direct detection of the NSs, and we can interpret their angular frequency, magnetic field. However, none of them have been detected so far by aLIGO, aVIRGO, which suggests that those NSs are very challenging to detect. We suggest this is mainly because the GW amplitude decays significantly due to the decay of Ω, χ and magnetic field, which can be seen from the results of Section 3. We have used the XNS code to determine the structure of magnetized, rotating NSs. We have calculated the timescale, after which the NS does not behave like a pulsar anymore due to dipole and GW radiation emitted by the NS. We have shown how GW strain decreases with time due to the Ω and χ decay, considering the magnetic field to remain constant during the process, which is a valid approximation, As we have seen from Fig. 8, the timescale at which magnetic field decays significantly is much longer ($\sim10^5$ yr) than those of Ω and χ, which is discussed in more detail in [16]. In contrast, we can argue that long before magnetic field decay changes GW wave amplitude, the NS stops behaving as a pulsar and thus will not be detectable anymore. If the NSs are poloidally dominated, χ decays very fast, so they cannot be detected for a longer duration by any of the detectors. However, if the NSs are toroidally dominated they can be detected by the detectors for a long time. We have calculated the cumulative SNR in Section 4 for toroidally dominated NSs, which may not be detected

Table 3. Change of GW strain (h) for toroidally dominated NS with $\rho_c = 10^{15}$ g cm^{-3}, due to Ω and χ decay

t, yr	M ($M_\odot$)	R_E, km	$B_{\max}$, G	ν, Hz	ME/GE	KE/GE	$\lvert\epsilon\rvert$	h (d = 10 kpc)
0	1.91	12.65	3.5×10^{17}	200	3.2×10^{-2}	6.6×10^{-3}	0.007	7.4×10^{-24}
50	1.907	12.65	3.5×10^{17}	138	3.2×10^{-2}	2.7×10^{-3}	0.007	4.4×10^{-25}

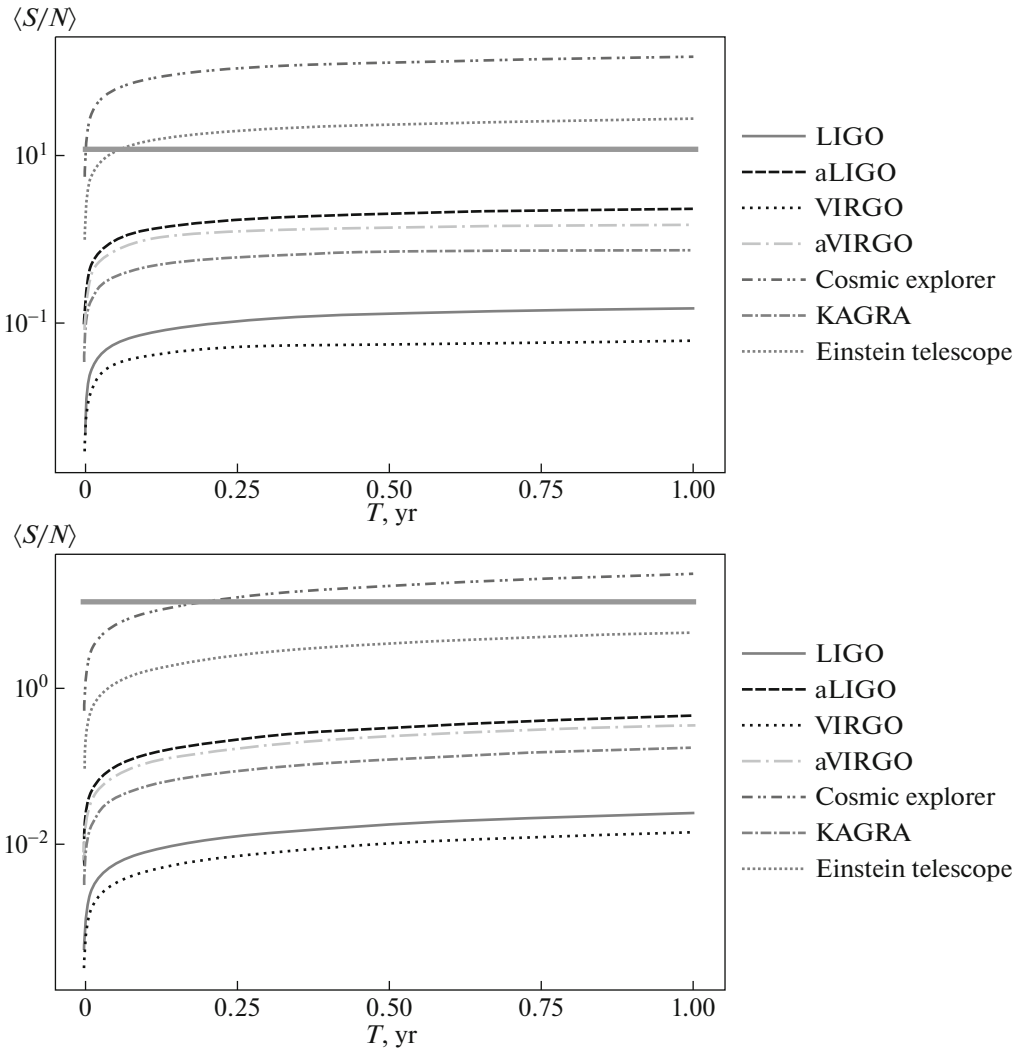

Fig. 7. SNR for various detectors as a function of integration time for a toroidal magnetic field dominated NS with initial $\chi = 3°$, initial $\nu = 200$ Hz, $B_{max} = 3.5 \times 10^{17}$ G (top panel), and $\nu = 200$ Hz, $B_{max} = 1.2 \times 10^{17}$ G (bottom panel), for two cases from Table 2. The horizontal line corresponds to $\langle S/N \rangle = 12$.

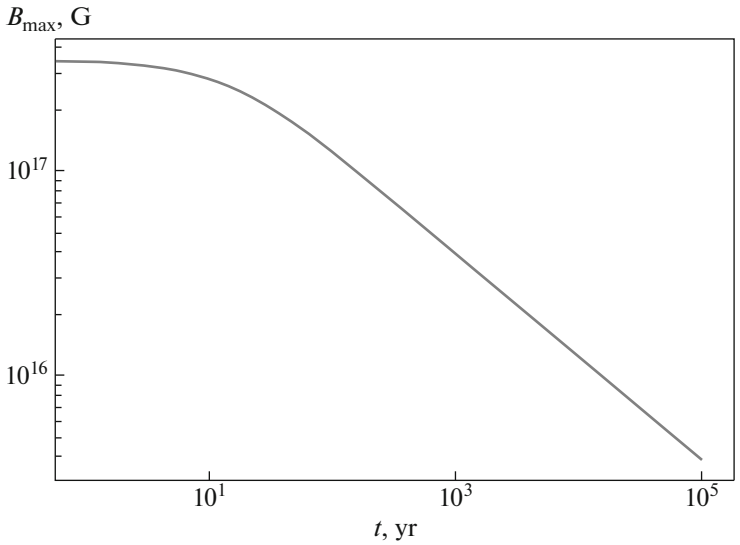

Fig. 8. Maximum magnetic field as a function of time of a toroidally dominated NS of mass $M = 2M_{\odot}$ with $\nu = 200$ Hz and initial $B_{max} = 3.5 \times 10^{17}$ G.

instantaneously, but can be detected by CGW detectors in 1 yr of integration time.

ACKNOWLEDGMENTS

The authors thank Surajit Kalita of the University of Cape Town for the discussion about extracting ellipticity with *XNS* code and about the time-stacking method to calculate cumulative SNR. They also thank Priti Gupta of Indian Institute of Science for comments.

FUNDING

This research was supported by the Prime Minister's Research Fellows (PMRF) scheme.

CONFLICT OF INTEREST

The authors of this work declare that they have no conflicts of interest.

REFERENCES

1. B. P. Abbott, R. Abbott, T. D. Abbott, et al., Phys. Rev. Lett. **116**, 131103 (2016).
2. B. P. Abbott, R. Abbott, T. D. Abbott, et al., Astrophys. J. Lett. **896**, L441048 (2020).
3. M. Zimmermann and E. Szedenits, Phys. Rev. D **20**, 351 (1979).
4. O. J. Piccinni, P. Astone, S. D'Antonio, S. Frasca, et al., Phys. Rev. D **101**, 082004 (2020).
5. S. Bonazzola and E. Gourgoulhon, Astron. Astrophys. **312**, 675 (1996).
6. A. G. Pili, N. Bucciantini, and L. Del Zanna, Mon. Not. R. Astron. Soc. **439**, 3541 (2014).
7. W. Y. Chau and R. N. Henriksen, Astrophys. J. Lett. **161**, L137 (1970).
8. S. Kalita, B. Mukhopadhyay, T. Mondal, and T. Bulik, Astrophys. J. **896**, 69 (2020).
9. D. T. Wickramasinghe, C. A. Tout, and L. Ferrario, Mon. Not. R. Astron. Soc. **437**, 675 (2014).
10. M. Sieniawska and M. Bejger, Universe **5**, 217 (2019).
11. P. R. Brady and T. Creighton, Phys. Rev. D **61**, 082001 (2000).
12. C. Cutler, I. Gholami, and B. Krishnan, Phys. Rev. D **72**, 042004 (2005).
13. M. Maggiore, *Gravitational Waves,* Vol. 1: *Theory and Experiments, Oxford Master Series in Physics* (Oxford Univ. Press, Oxford, 2007).
14. C. J. Moore, R. H. Cole, and C. P. L. Berry, Class. Quantum Grav. **32**, 015014 (2014).
15. S.-J. Huang, Y.-M. Hu, V. Korol, et al., Phys. Rev. D **102**, 063021 (2020).
16. M. Das and B. Mukhopadhyay, Astrophys. J. (2023, in press); arXiv: 2302.03706.